

Foundation Soil Stability of Immersed Tunnel Subjected to High Speed Train

Sun Xiaojing^{*}, Liu Weining

*School of Civil & Architecture Engineering, Beijing Jiaotong University
Beijing 100044, China*

* e-mail: xjsun1@bjtu.edu.cn; littlemirror@126.com

ABSTRACT

The effect on the base of a railway immersed tunnel by the high speed train was studied in this paper. The liquefaction of the tunnel sand foundation under the water was estimated by using the method of numerical simulation. It is found that there will be very large capacity in the sand foundation to endure the periodical load of high speed train.

KEYWORDS: immersed foundation; high speed railway; train dynamic loads; liquefaction analysis

INTRODUCTION

Under the action of the dynamical loads, saturated sand, poorly graded saturated gravel sand and saturated light loam usually have large deformation. And they may suddenly lose their strength and turn into a phase similar to liquid, which will lead to a seriously damage consequence. Therefore, the study of the liquefaction of the saturated gravel sand is an important problem in geotechnical engineering. Part of the foundation soil under the planning immersed tunnel through Yanzi River at Nanjing for the high speed railway from Beijing to Shanghai is in the range of liquefaction. It has been proved by gradation test that the foundation soil has a possibility of liquefaction. But whether it will liquefy under the frequent action of the high speed train is still a question worth to study. In this paper, it will be studied by using the method of numerical simulation.

DETERMINATION OF ANALYTICAL PARAMETERS

Determination of Typical Analytical Sections

The immersed tunnel for high speed train will be 2090m across Yanzi River in Nanjing. Several typical cross sections is used to study the stability of the immersed tunnel foundation. It will mostly considered for the scope of distribution and the depth of overlay of fine sand and silt sand, because they are the main factors affecting on the liquefaction ability of the foundation. This study is based on the following three typically analytical cross sections, as shown in Fig.1.

- (1) Section A-A: at the tunnel shaft in the north of the river, Mileage: CK340+690, Drill hole: CZ-JT2.
- (2) Section B-B: at the maximum water-depth place, Mileage: CK341+310, Drill hole: CZ-JT6.
- (3) Section C-C: at the tunnel shaft in the south of the river, Mileage: CK342+232, Drill hole: CZ-JT16.

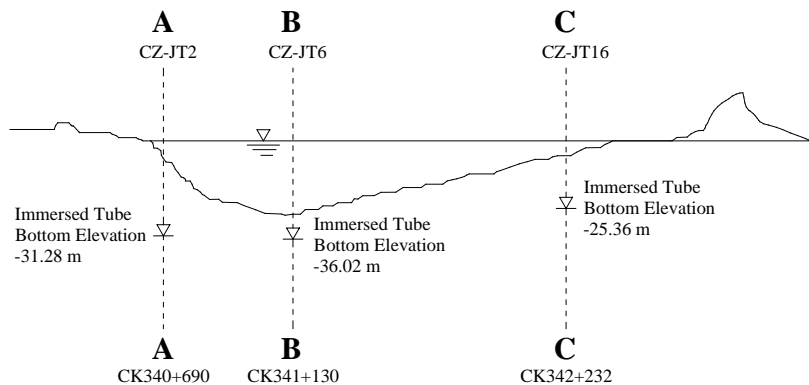


Figure 1: Location of three typically analytical cross sections

Determination of Parameter

Determination of ground dynamic assumed parameter

The dynamic parameters of the three analytical cross sections are determined based on *The experimental report of the soil dynamic property*^[1]. According to the report^[1], the soils are further stratified according to actual soil thickness or sampling location depth to reflect accurately the change of soil dynamic modulus and damping ratio in the analytic process. The main soil parameters of Section B-B are shown in Table 1.

Determination of the minimum soil liquefaction shear stress

The minimum liquefaction shear stress of immersed foundation is determined according to *The Report*^[1]. The estimated curves of the minimum liquefaction shear stress level of sand corresponding to three equivalent vibrating number ($N < 10$, $10 < N < 30$, $N > 30$) are shown in Fig. 2.

Table 1: Main soil parameter of section B-B

Soil depth /m	Stress ratio Kc	γ	$G / (\times 10^4 \text{kPa})$	λ	c / kPa	$\phi / (^\circ)$
0-5			5.591			
5-9			8.469	0.040	0	21.3
9-16			13.912	0.052	0	27.2
16-20	1.5	1.0×10^{-4}	14.498			
20-25			16.010			
25-30			17.597	0.030	0	34
30-35			19.259			
35-40			20.409			

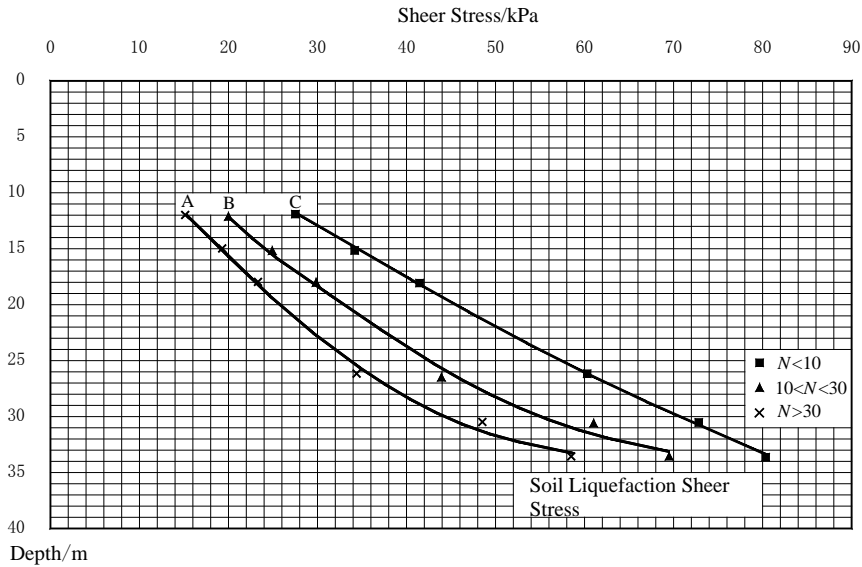


Figure 2: Foundation liquefaction shear stress

The liquefaction shear stress $[\tau]$ in Fig. 2 can be written as

$$[\tau] = \gamma \cdot h \cdot C_r \cdot \left[\frac{\sigma_d}{2\sigma_3} \right] \tag{1}$$

where τ is soil gravity, h is the depth of embedment, $\left[\frac{\sigma_d}{2\sigma_3} \right]$ is liquefaction shear stress ratio as

shown in Table 3, C_r is a factor which is used to correct the triaxial test data to reflect the site actual state of stress and it is obtained by test.

Liquefaction shear stress ratio $\left[\sigma_d / 2\sigma_3 \right]$ of different soil depth is shown in Table 2.

Table 2: Liquefaction shear stress ratio $\left[\sigma_d / 2\sigma_3 \right]$

$K_c=1.5, \sigma_3=300\text{kPa}$				
Fine sand 1 (12-19m)	$Dr = 0.7, Cr = 0.66$	$N < 10$	$10 < N < 30$	$30 < N$
		0.179	0.130	0.102
Rock flour (20-30m)	$Dr = 0.77, Cr = 0.69$	$N < 10$	$10 < N < 30$	$30 < N$
		0.194	0.173	0.134
Fine sand 2 (beyond 31m)	$Dr = 0.65, Cr = 0.69$	$N < 10$	$10 < N < 30$	$30 < N$
		0.179	0.155	0.136

Based on the Table 2, the relationship between the liquefaction shear stress level $\left[\tau_i \right]$ and the corresponding liquefaction vibrating number N_{if} is obtained by regression analysis, as shown in Table 3 and Fig. 3.

The equivalent liquefaction vibrating number N_e vibration shear stress in soil due to the train vibration is determined based on the above relationship. Accordingly, it can be used to determine the corresponding liquefaction shear stress rate under the train vibration.

Table 3: Relationship between liquefaction shear stress ratio and liquefaction vibrating number

Fine sand 1 (12-19m)	$N_{if} = 945.57 \exp(-0.1734[\tau_i])$
Rock flour (20-30m)	$N_{if} = 1756.8 \exp(-0.0736[\tau_i])$
Fine sand 2 (beyond 31m)	$N_{if} = 2558.8 \exp(-0.0521[\tau_i])$

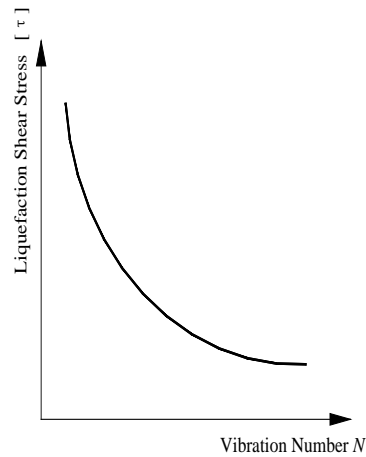


Figure 3: Relationship between liquefaction shear stress ratio and liquefaction vibrating number

WHOLE STABILITY OF IMMERSED TUNNEL DUE TO HIGH SPEED TRAIN'S VIBRATION LOADS

High Speed Train's Load Simulation

The high speed train's loads are determined on the basic of vehicle/track coupling dynamic model, as shown in Fig.4. The locomotive and train parameters of the train model are determined based on *The report of study of high speed experimental train (96J01)* of the china railway scientific and technical development plan in 2000.

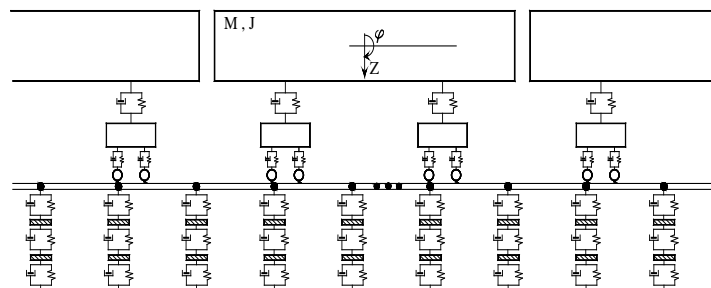


Figure 4: Vehicle/Track coupling dynamic model

The rail track in the tunnel is integer structured with rail supported by elastic block and 1760 sleepers per kilometers. The wheel-rail contact stiffness is $1.4E6KN/m^{[2]}$. And the parameters of rail

track are shown in Table 4, where the damping factors of structure under track are referred to Reference [3] and [4].

The track vertical irregularity is assumed as function (2)^[2]

$$\delta(x) = A_0 \cdot [1.0 - \exp(-x/L_x)^3] \cdot \sin(2\pi/L_0) \quad (2)$$

where $A_0 = 0.6\text{cm}$ is the amplitude of irregularity^[3]; $L_0=10\text{m}$ is the wave length of irregularity^[3]; $L_x = 5\text{m}$ is the position of the maximum peak value of irregularity.

Table 4: Assumed parameter of steel rail and rail bearing^[2,3]

	Mass of Vibration/kg	Damping of Vibration/ (kNs • m ⁻¹)	Stiffness of Vibration/ kN
Steel rail	7830/m ³		2.06E8
Rail rubber pad	2.0	75.0	70000.0
C50 Supporting block	100	300.0	7000000.0
Rail rubber pad under supporting block	5.0	90.0	66000.0

From the model mentioned above, the dynamical loads^[5,6] on the track bed of immersed tunnel can be obtained. The corresponding load spectra resulted from high speed train at 100km/h, 150km/h, 200km/h, 250km/h, 300km/h, 350km/h six kinds of speed. The main character values are shown in Table 5.

Table 5: Simulation maximum load of monolithic track bed train (axial dynamical load)

Train speed/ (km • h ⁻¹)	Maximum dynamical train Load/ (kN • h ⁻¹)	Maximum dynamical locomotive load/ (kN • m ⁻¹)	Frequency bandwidth/ Hz	Maximum spectrum frequency/ Hz
100	87	118.66	0~15	3.1
150	88	121.84	0~30	1.5
200	86	121.05	0~35	2.1
250	95	125.74	0~40	7.8
300	100	133.82	0~46	9.4
350	109	145.4	0~55	10.7

Result of Vibration Sheer Stress of Foundation due to High Speed Train

Determination of maximum sheer stress location

Stress distribution mode in tube foundation of dynamical loads due to train's vibration is unknown. The maximum horizontal and vertical sheer stress distribution mode in tube foundation was studied. When the train's velocity $V=350\text{km/h}$, the distribution of maximum horizontal sheer stress at the immersed tube bottom is shown in Fig. 5, and the same to the other velocity. According to this, the location of maximum sheer stress in the foundation due to train dynamical load can be pointed at point J of the immersed tube bottom.

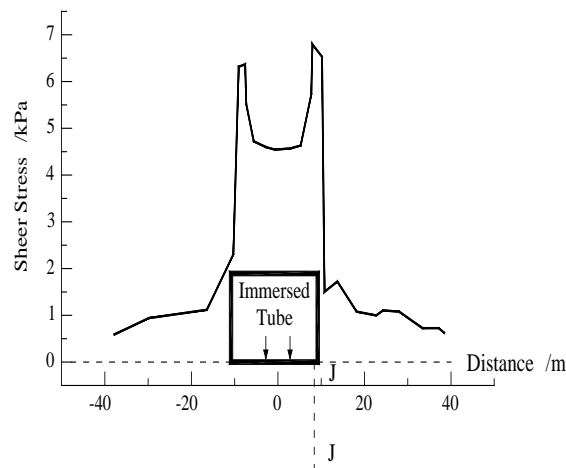


Figure 5: Horizontal distribution of maximum sheer stress at elevation of immersed tube bottom

So the sheer stress distribution on perpendicular line J-J through point J is made to analyze for different train speed, which is the distribution of maximum dynamical sheer stress in the foundation due to train vibration. Accordingly, the stability determination of immersed foundation by high speed train can be gained compared with the liquefaction sheer stress of foundation.

Maximum sheer stress of the line J-J

The distribution of maximum sheer stress on the line J-J under the immersed tube, which is at the section A-A, B-B, C-C, corresponding to six velocity, can be gained based on the elastic-plastic time-history FEM analysis of train vibration. The comparison is shown in Fig. 6, which is the distribution between the maximum sheer stress and the liquefaction sheer stress at section B-B under 150km/h. And it is the same to the other sections under six train velocities.

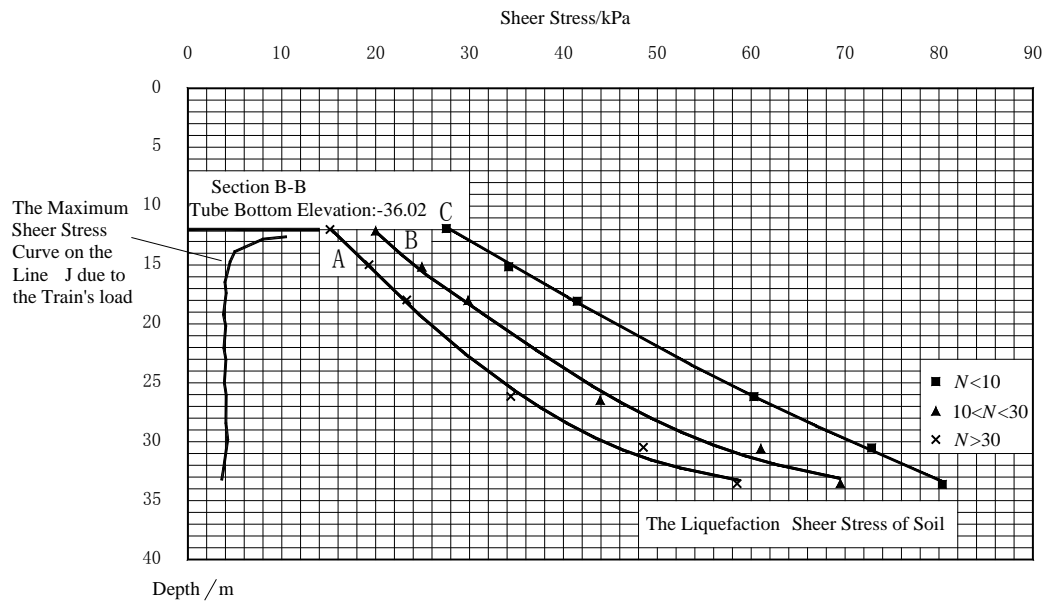


Figure 6: Maximum shear stress and foundation liquefaction shear stress on line J due to train vibration

Determination of the equivalent vibrating time of the shear stress by the train's vibration

The maximum shear stress in the foundation due to the train's vibration is smaller than the liquefaction shear stress, as shown in Fig. 6. In order to confirm the standard of soil liquefaction, the equivalent vibrating time of the dynamical shear stress under the immersed tube should be calculated. And this equivalent vibrating time N_e can be written as equation (3)^[8]

$$N_e = N_{mf} \cdot \sum \frac{N_i}{N_{if}} \quad (3)$$

where N_{mf} is the corresponding liquefaction vibrating time when τ_m is the average shear stress; N_{if} is the corresponding liquefaction vibrating time when τ_i is the No. i shear stress level. This corresponding relationship is gained through the regression analysis based on the data of *The Report*^[1], as shown in Table 4 and Fig. 3. In this study, the corresponding equivalent vibrating times of all the shear stress time-history due to the train's vibration are calculated. The result indicates that the equivalent vibrating times of shear stress under the immersed tube are smaller than 15. So the soil liquefaction shear stress in the range of $10 < N < 30$ should be chosen as the standard of soil liquefaction, as the line B shown in Fig. 6.

CONCLUSIONS

The distribution of the maximum dynamic shear stress at the bottom of immersed tube due to high speed train corresponding to six kinds of speed is obtained. The maximum shear stress is located at the immersed tube bottom at the maximum water-depth of tunnel (section B-B). The maximum dynamic shear stress at the bed next to the immersed tube is 10.6kPa, which is 53 percent of the soil liquefaction shear stress (20kPa, $10 < N < 30$, as shown in Fig. 6).

According to the shear stress time-history curve of vibration which is gained by this study, the immersed tunnel foundation will not be liquefied by high speed train's vibration, and there is a rather large surplus (safety factor $k = 20 \text{ kPa} / 10.6 \text{ kPa} = 1.89$).

ACKNOWLEDGMENTS

The results presented in this paper have been obtained within the frame of "Study on environmental vibration induced by urban mass transit and control measures". The project is funded by the National Natural Science Foundation of China (50538010).

This research was supported by the National Natural Science Foundation of China (51408033) and also by the Fundamental Research Funds for the Central Universities (2016JBM046).

REFERENCES

1. The survey and design institute of major bridge engineering bureau of ministry of China railway and the Center of forecasting and analysis of China University of Geosciences. The experimental report of the soil dynamic property. Wuhan: China Zhongtie Bridge Engineering Group, 1997
2. Lei Xiaoyan, The Numerical Analytical Method of Railway Track Structure. Beijing: China Railway Publishing House, 1998
3. No 3 prospecting and design institute of China railway department. The temporary regulations of design or track, bridge, tunnel, station, etc. for Jing-Hun high speed railway, 1998
4. Ir A P de Man. Determination of dynamic track properties by means of excitation hammer testing. Rail Eng Int Edition, 1996, 4: 8-9
5. College of Civil Engineering and Architecture, Northern Jiaotong University. The study of the whole stability of the immersed tunnel due to seismic and train's vibration loads(project 96G13-D), 1998

6. Liu Weining, Xia He. The environment response of subway train's vibration. *Chinese Journal of Rock Mechanics and Engineering*, 1996,15: 586-593
7. Pan Changshi, Liu Weining, The test and dynamic analysis of tunnel train vibration. *Journal of Lanzhou Railway Institute*, 1985, 4(2):1-21
8. Wu Shiming, et al. *Soil Dynamics*. Beijing: China Architecture & Building Press, 2000
1. Jian Han, Guotang Zhao, Xinbiao Xiao, Zefeng Wen, Xuesong Jin: "Contact Behavior between Slab Track and its Subgrade under High-Speed Train Loading and Water-Soil Interaction" *Electronic Journal of Geotechnical Engineering*, 2015 (20.2) pp 709-722. Available at ejge.com
2. Xiaojun Dai, Jianjun Liu, and Yuan Li: "Analysis of Roadbed Deformation Monitoring of Cangzhou Section of Beijing to Shanghai Express Railway" *Electronic Journal of Geotechnical Engineering*, 2015 (20.2) pp 814-. Available at ejge.com



© 2016 ejge

Editor's note.

This paper may be referred to, in other articles, as:

Sun Xiaojing and Liu Weining: "Foundation Soil Stability of Immersed Tunnel Subjected to High Speed Train" *Electronic Journal of Geotechnical Engineering*, 2016 (21.12), pp 4359-4368. Available at ejge.com.